

Positron emission tomography imaging of the 18-kDa translocator protein (TSPO) with [^{18}F]FEMPA in Alzheimer's disease patients and control subjects

Andrea Varrone · Vesa Oikonen · Anton Forsberg · Juho Joutsa · Akihiro Takano · Olof Solin · Merja Haaparanta-Solin · Sangram Nag · Ryuji Nakao · Nabil Al-Tawil · Lisa A. Wells · Eugenii A. Rabiner · Ray Valencia · Marcus Schultze-Mosgau · Andrea Thiele · Sonja Vollmer · Thomas Dyrks · Lutz Lehmann · Tobias Heinrich · Anja Hoffmann · Agneta Nordberg · Christer Halldin · Juha O. Rinne

Received: 23 May 2014 / Accepted: 29 October 2014 / Published online: 21 November 2014
© Springer-Verlag Berlin Heidelberg 2014

Abstract

Purpose Imaging of the 18-kDa translocator protein (TSPO) is a potential tool for examining microglial activation and neuroinflammation in early Alzheimer's disease (AD).

Andrea Varrone and Vesa Oikonen contributed equally to this work.

Electronic supplementary material The online version of this article (doi:10.1007/s00259-014-2955-8) contains supplementary material, which is available to authorized users.

A. Varrone · A. Forsberg · A. Takano · S. Nag · R. Nakao · C. Halldin

Karolinska Institutet, Department of Clinical Neuroscience, Centre for Psychiatry Research, Stockholm, Sweden

V. Oikonen · J. Joutsa · O. Solin · M. Haaparanta-Solin · J. O. Rinne
Turku PET Centre, University of Turku, Turku, Finland

N. Al-Tawil
Karolinska Trial Alliance, Karolinska University Hospital, Stockholm, Sweden

L. A. Wells · E. A. Rabiner
Imanova Centre for Imaging Sciences, London, UK

R. Valencia · M. Schultze-Mosgau · A. Thiele · S. Vollmer · T. Dyrks · L. Lehmann · T. Heinrich · A. Hoffmann
Bayer Healthcare AG, Berlin, Germany

A. Nordberg
Department of Geriatric Medicine, Karolinska University Hospital Huddinge, Stockholm, Sweden

A. Varrone (✉)
Karolinska Institutet, Department of Clinical Neuroscience, Centre for Psychiatry Research, Karolinska Hospital, R5:02, SE-17176 Stockholm, Sweden
e-mail: andrea.varrone@ki.se

[^{18}F]FEMPA is a novel high-affinity second-generation TSPO radioligand that has displayed suitable pharmacokinetic properties in preclinical studies. The aims of this study were to quantify the binding of [^{18}F]FEMPA to TSPO in AD patients and controls and to investigate whether higher [^{18}F]FEMPA binding in AD patients than in controls could be detected in vivo.

Methods Ten AD patients (five men, five women; age 66.9 ± 7.3 years; MMSE score 25.5 ± 2.5) and seven controls (three men, four women; age 63.7 ± 7.2 years, MMSE score 29.3 ± 1.0) were studied using [^{18}F]FEMPA at Turku (13 subjects) and at Karolinska Institutet (4 subjects). The in vitro binding affinity for TSPO was assessed using PBR28 in a competition assay with [^3H]PK11195 in seven controls and eight AD patients. Cortical and subcortical regions of interest were examined. Quantification was performed using a two-tissue compartment model (2TCM) and Logan graphical analysis (GA). The outcome measure was the total distribution volume (V_T). Repeated measures analysis of variance was used to assess the effect of group and TSPO binding status on V_T .

Results Five AD patients and four controls were high-affinity binders (HABs). Three AD patients and three controls were mixed-affinity binders. V_T estimated with Logan GA was significantly correlated with V_T estimated with the 2TCM in both controls ($r=0.97$) and AD patients ($r=0.98$) and was selected for the final analysis. Significantly higher V_T was found in the medial temporal cortex in AD patients than in controls ($p=0.044$) if the TSPO binding status was entered as a covariate. If only HABs were included, significantly higher V_T was found in the medial and lateral temporal cortex, posterior cingulate, caudate, putamen, thalamus and cerebellum in AD patients than in controls ($p<0.05$).

Conclusion [^{18}F]FEMPA seems to be a suitable radioligand for detecting increased TSPO binding in AD patients if their binding status is taken into account.

Keywords Neuroinflammation · Microglia · Translocator protein · Dementia · Alzheimer

Introduction

Neuroinflammation is a pathological phenomenon characterized by microglial activation and reactive astrogliosis. Neuroinflammatory changes are observed in various neurodegenerative disorders including Alzheimer's disease (AD). Post-mortem studies in AD patients have shown that microglial activation is associated with the presence of amyloid plaques [1], suggesting a link between amyloid pathology and neuroinflammation. In vivo imaging of microglial activation can be a useful tool for early detection of neuroinflammation in AD. The 18-kDa translocator protein (TSPO) is a mitochondrial protein [2, 3] expressed in macrophages [4], microglia [5] and reactive astrocytes [6], and is considered a marker of activated microglia and macrophages [7]. ((*R*)-1-(2-chlorophenyl)-*N*- ^{11}C -methyl-*N*-(1-methylpropyl)-3-isoquinoline carboxamide ([^{11}C](*R*)-PK11195) was the first TSPO radioligand developed for imaging activated microglia. The first evidence of increased TSPO binding in AD patients using [^{11}C](*R*)-PK11195 was reported by Cagnin et al. [8]. This finding was replicated in a group of 13 AD patients who were also examined with the amyloid radioligand [^{11}C]PIB [9]. A large overlap of TSPO binding signal was, however, observed between controls and patients with AD or with mild cognitive impairment (MCI) using [^{11}C](*R*)-PK11195 [10, 11]. It was suggested that either microglial activation in AD is a subtle phenomenon [11] or that [^{11}C](*R*)-PK11195 is not sensitive enough to detect in vivo increased microglial activation in AD [10].

Several TSPO radioligands with greater affinity than [^{11}C](*R*)-PK11195 have been developed [12], and some of them have been used for in vivo imaging of neuroinflammation. Increased TSPO binding in AD and MCI patients compared with controls has been found using the high-affinity radioligand *N*-(2,5- ^{11}C -dimethoxybenzyl)-*N*-(5-fluoro-2-phenoxyphenyl)acetamide ([^{11}C]DAA1106) [13, 14]. When the ^{18}F analogue of DAA1106, *N*-(5-fluoro-2-phenoxyphenyl)-*N*-(2- ^{18}F -fluoroethyl-5-methoxybenzyl)acetamide ([^{18}F]FEDAA1106) was used, no statistically significant increase in TSPO binding in AD patients could be detected in comparison with controls [15]. A large variability in outcome measures of [^{18}F]FEDAA1106 among different subjects was observed [15].

A major source of variability in TSPO binding is related to the presence of different binding affinity profiles. This

property was first demonstrated and fully examined for the high-affinity TSPO radioligand (*N*-{[2-(methoxy)phenyl]methyl}-*N*-[4-(phenoxy)-3-pyridinyl]acetamide (PBR28) [16], but it was also shown for other second-generation TSPO ligands [17]. In the case of [^{11}C]PBR28, it has been demonstrated that the *rs6971* polymorphism of the TSPO gene is responsible for the different binding affinity profiles [18]. Subjects can be high-affinity, mixed-affinity or low-affinity binders (HAB, MAB, LAB) based on the homozygosity or heterozygosity for the polymorphism. Therefore, imaging of the TSPO using second-generation radioligands should take into account the binding status of the study participants, particularly when different groups of subjects are examined. Recently, increased TSPO binding in amyloid-positive AD patients has been demonstrated using [^{11}C]PBR28 and adjusting for TSPO genotype [19].

N-{2-[2- ^{18}F -Fluoroethoxy]-5-methoxybenzyl}-*N*-[2-(4-methoxyphenoxy)pyridine-3-yl]acetamide ([^{18}F]FEMPA, CAS 1207345-42-3) is an aryloxyppyridylamide derivative that is less lipophilic than [^{18}F]FEDAA1106, and preclinical data in nonhuman primates showed fast elimination from the brain and better signal-to-noise ratio. Based on these initial preclinical findings suggesting favourable kinetic properties of [^{18}F]FEMPA, it was decided to move forward with the characterization of the radioligand in human subjects. [^{18}F]FEMPA was considered to be a potential ^{18}F -labelled TSPO radioligand with similar kinetic properties (rapid wash-out from the brain and high target-to-background ratio) as the ^{11}C -labelled TSPO tracer PBR28. The aims of the present study were therefore to quantify the in vivo binding of [^{18}F]FEMPA to TSPO in AD patients and controls and to investigate whether increased binding of [^{18}F]FEMPA to the TSPO could be demonstrated in AD patients in vivo.

Materials and methods

Subjects

The study was conducted in line with the principles of the Helsinki Declaration and approved by FIMEA and the Swedish Medical Products Agency, by the local Ethics Committee of the Southwest Hospital District of Finland and of the Stockholm region, and by the Radiation Safety Committee of Turku Hospital and Karolinska University Hospital. The study was registered at www.ClinicalTrials.gov (NCT01153607) and included a total of 24 participants. Of these participants, 17 were included in the present study and 7 were included in a whole-body dosimetry study that will be reported separately.

Ten AD patients and seven controls were studied at Turku PET Centre (13 subjects) and at Karolinska Institutet (4 subjects; Table 1). All subjects gave written informed consent for

Table 1 Details of controls and AD patients and their binding status

Subjects	Centre	Gender	Age (years)	MMSE score	Binding status	Treatment
Control 1	Turku	M	66	28	HAB	–
Control 2	Turku	F	56	29	MAB	–
Control 3	Turku	M	55	30	MAB	–
Control 4	Turku	F	69	30	HAB	–
Control 5	Turku	F	71	28	HAB	–
Control 6	Karolinska Institutet	M	58	30	MAB	–
Control 7	Karolinska Institutet	F	71	30	HAB	–
			Mean ± SD 64±7	Mean ± SD 29.3±1.0		
AD 1	Turku	M	74	23	– ^a	Rivastigmine 9.5 mg daily
AD 2	Turku	F	56	29	– ^a	Donepezil 10 mg daily
AD 3	Turku	M	69	28	HAB	Rivastigmine 9.5 mg daily
AD 4	Turku	M	55	25	MAB	Donepezil 10 mg daily
AD 5	Turku	F	67	26	HAB	Rivastigmine 9.5 mg daily
AD 6	Turku	F	76	24	HAB	Donepezil 10 mg daily
AD 7	Turku	F	67	22	MAB	Donepezil 5 mg daily
AD 8	Karolinska Institutet	F	71	27	HAB	Donepezil 5 mg daily
AD 9	Karolinska Institutet	M	61	28	MAB	Galantamine 16 mg daily
AD 10	Turku	M	73	23	HAB	Donepezil 10 mg daily
			Mean ± SD 67±7	Mean ± SD 25.5±2.5*		

HAB high-affinity binder, MAB mixed-affinity binder

* $p=0.002$ vs. controls, two-tailed unpaired t test

^a Plasma not available (AD2 only 10 min of blood data available)

participation in the study. AD patients were recruited from the University of Turku and from the Karolinska University Hospital, Huddinge. Controls were recruited at both sites, by local advertisement and from a database at the Karolinska Trial Alliance in Stockholm. All subjects underwent careful clinical and neurological examinations, Mini-Mental State Examination (MMSE), and neuropsychological testing including assessment of memory function. Probable AD was diagnosed according to the clinical criteria of the National Institute of Neurological and Communicative Disorders and Stroke and Alzheimer's Disease and Related Disorders Association (NINCDS-ADRDA) and the criteria of the Diagnostic and Statistical Manual of Mental Disorders (DSM IV). In addition to these criteria, the diagnostic criteria defined by McKhann et al. that include imaging or CSF and in vivo biomarkers were used [20], particularly in those patients showing unimpaired global cognition (MMSE score 28, 29 and 30).

The inclusion criterion was mild to moderate disease (MMSE score ≥ 20 and a Clinical Dementia Rating score of 1 or 2). Other forms of dementia (e.g. dementia with Lewy bodies) had to be excluded. Patients were under stable treatment (at least 6 months before the study) with cholinesterase inhibitors. Additionally, neither AD patients nor controls were allowed to show signs of systemic autoimmune or inflammatory disease. Participants with other current treatments acting

on the central nervous system (including anti-inflammatory treatments in prespecified time frames) were also excluded in order to avoid interference with the in vivo binding of the radioligand.

PET experimental procedures

Details of radiolabelling procedures of [^{18}F]FEMPA are described in Supplementary Appendix 1. Specific radioactivity at the time of injection was between 31 and 1,343 GBq/ μmol . The injected radioactivity was 251 ± 16 MBq in controls and 251 ± 10 MBq in AD patients. The injected mass was 0.68 ± 0.97 μg (range 0.07 – 2.55 μg) in controls and 0.67 ± 1.16 μg (range 0.09 – 3.74 μg) in AD patients. There were no significant adverse or clinically detectable pharmacological effects in any of the 17 subjects. No significant changes in vital signs or the results of laboratory studies or electrocardiograms were observed.

PET measurements

PET measurements were performed using an ECAT EXACT HR+ (Turku PET Centre) and an ECAT EXACT HR (Karolinska Institutet) systems in two PET sessions. The first PET session consisted of a 90-min dynamic acquisition with a

series of frames of increasing duration (6×5 s, 3×10 s, 2×20 s, 4×60 s, 6×180 s, 11×360 s). The second PET session of 30 min was performed between 120 and 150 min after radioligand injection and consisted of five frames of 360 s. A transmission scan of 5 min was acquired before each dynamic acquisition using three rotating ^{68}Ge sources. At Turku, images were reconstructed with filtered back projection, a 256×256 matrix, and a pixel size of 1.226×1.226 mm. At Karolinska Institutet, images were reconstructed with filtered back projection, with a 2-mm Hanning filter, a zoom factor of 2.17, and a 128×128 matrix. Images were corrected for attenuation and scatter. A NEMA Jaszack phantom with spheres of different diameter and uniform background filled with ^{18}F radioactive solution at a ratio of about 4:1 was acquired at both centres under similar experimental conditions and using the standard reconstruction method at each centre. The difference in the recovery coefficient between the two PET systems was 9.4 % for the spheres and 4.2 % for the background, suggesting the possibility that the data from the two PET systems could be pooled.

Arterial blood was sampled using an automated system (Allogg AB, Mariefred, Sweden) for the first 10 min and using manual sampling thereafter. Samples for metabolite analysis (HPLC, Supplementary Appendix 1) were taken at 2, 5, 10.5, 20, 30, 45, 60, 90, 120 and 150 min.

Magnetic resonance imaging

MRI was performed at Turku University using a Philips Gyroscan Intera 1.5-T Nova Dual scanner (Philips, Best, The Netherlands) and at the Karolinska Institutet using a 1.5-T GE Signa system (GE Healthcare, Milwaukee, WI). MRI scans consisted of a T2-weighted sequence for ruling out pathological changes and a 3-D T1-weighted spoiled gradient recalled (SPGR) sequence for both coregistration with PET and volume of interest (VOI) analysis. MRI scans were evaluated for white matter changes according to the Age-Related White Matter Changes (ARWMC) scale [21], and exclusion criteria were an ARWMC score of >1 in the basal ganglia and >2 in the subcortical white matter.

Image analysis

Images were analysed at Turku PET Centre. PET images were coregistered to the T1-weighted MRI images using SPM2 (Wellcome Department of Imaging Neuroscience, London, UK). VOIs were delineated using the software Imadeus 1.20 (Forima, Turku, Finland). The following regions were defined: frontal cortex, parietal cortex, lateral and medial temporal cortex, occipital cortex, posterior cingulate cortex, caudate, putamen, thalamus, pons, cerebellum and the subcortical white matter.

TSPO binding status

The TSPO binding status was measured at Imanova Centre for Imaging Sciences from peripheral blood samples. In two AD patients (AD1 and AD2) plasma was not available for the binding competition assay. The PBR28 binding status was measured using a competition binding assay with [^3H]PK11195 on platelet membrane suspension (Supplementary Appendix 2). Data were analysed using GraphPad Prism 5.0 software. One-site and two-site binding models were compared using a sum-of-square F test. In four subjects (controls 6 and 7, AD patients 8 and 9) the binding status was less reliably measured because of low protein concentration in the samples.

Data analysis

A preliminary analysis showed that the first PET session was sufficient for quantification of [^{18}F]FEMPA binding. Therefore, only 90 min of data were used for the final analysis. The radioactivity concentrations in the different brain regions were reported as standard uptake values (SUV) calculated as: $\text{SUV} = (\text{kBq}\cdot\text{cm}^{-3}/\text{Bq injected})/\text{body weight (g)}$. Two parameters were measured to assess the kinetic properties of [^{18}F]FEMPA: the time to peak uptake (t_{peak}) and the time when the brain radioactivity decreased to 50 % of the peak ($t_{\text{half-peak}}$), both expressed in minutes. The quantification was performed using kinetic and Logan graphical analysis (GA). Kinetic analysis was performed with nonlinear least squares fitting and a two-tissue compartment model (2TCM) with four parameters (K_1 , K_1/k_2 , k_3/k_4 , k_4) and blood volume fitted for each region. The outcome measure was the total distribution volume (V_T). In one subject (AD2), arterial blood sampling was not successful, and this patient was excluded from further analyses. The variability of V_T estimated with the 2TCM and Logan GA was calculated as the ratio between the standard deviation and the mean for each brain region, and expressed as percentage (coefficient of variance, COV%).

Statistical analysis

Regression analysis was used to assess the agreement between the 2TCM and Logan GA in estimating V_T . The F test was used to compare the variability of V_T (COV%) estimated with the 2TCM and Logan GA. Repeated measures analysis of variance (RM-ANOVA) was applied to test the effects of group (AD patients vs. controls) and TSPO binding status (MAB or HAB) on V_T . The brain region (VOI) was entered as within-subject factor, the group as between-subject factor and the TSPO binding status as covariate. RM-ANOVA was also applied only to the data from the HABs. In this case, no covariate was entered in the

model. As post-hoc analysis, ANOVA was applied to test the differences in V_T between AD patients and controls in different brain regions. Statistical significance was assumed at $p < 0.05$.

Results

TSPO binding status

Four controls were HABs and three were MABs, whereas five AD patients were HABs and three were MABs (Supplementary Appendix 2). No LABs were observed in either group. The value of K_i high for the HABs was 2.26 ± 0.18 nM. The values of K_i high and low for the MABs were 1.93 ± 0.75 nM and 189.8 ± 14.4 nM, respectively.

Radiometabolite analysis

$[^{18}\text{F}]$ FEMPA showed rapid metabolism in vivo with $<20\%$ of tracer present in plasma 20 min after injection and $<10\%$ after 90 min (Fig. 1 and Supplementary Figs. 1 and 2). There were no statistically significant differences in the parent fraction or

in the fraction of metabolites between controls and AD patients or between MABs and HABs (Fig. 1).

Kinetic properties of $[^{18}\text{F}]$ FEMPA

Representative SUV images and mean time–activity curves of $[^{18}\text{F}]$ FEMPA are presented in Figs. 2 and 3. In each binding group there were no statistically significant differences between controls and AD patients in kinetic parameters based on SUV data (Supplementary Table 1). However, among the AD patients the $t_{\text{half-peak}}$ was significantly lower in MABs than in HABs ($p = 0.008$), whereas only a trend was observed in the controls ($p = 0.15$).

PET quantification

A preliminary comparison between a one-tissue compartment model and the 2TCM showed that the 2TCM provided a better fit of the data by visual inspection and based on the Akaike information criterion. Therefore only the 2TCM was used in the final analysis of the data (Supplementary Fig. 3, Supplementary Tables 2 and 3). In HABs, V_T values were significantly higher ($p < 0.05$) in AD patients than in controls for the parietal cortex, lateral and medial temporal cortex, posterior cingulate, thalamus and cerebellum.

Representative Logan plots of $[^{18}\text{F}]$ FEMPA are presented in Fig. 4. There was a statistically significant correlation between V_T estimated with the 2TCM and with Logan GA in controls ($r = 0.97$, $p < 0.001$) and AD patients ($r = 0.98$, $p < 0.001$) across all regions and subjects, with values close to the line of identity (Supplementary Fig. 4). The mean COV% of V_T estimated with Logan GA tended to be lower than the mean COV% of V_T estimated with the 2TCM in AD patients ($p = 0.05$, Supplementary Table 4). Logan GA was selected for the final analysis of the data, considering the high correlation for V_T between Logan GA and the 2TCM and the slightly lower COV% of V_T estimated with Logan GA in AD patients.

RM-ANOVA using Logan V_T showed a significant effect of TSPO ($F = 17.3$, $p = 0.001$) and a significant region \times TSPO binding status interaction ($F = 5.2$, $p = 0.004$). The group showed only a nonsignificant trend ($F = 3.7$, $p = 0.077$). No statistically significant region \times group interaction was found. However, when only HABs were included in the analysis, a significant effect of group ($F = 9.2$, $p = 0.02$) was observed but no statistically significant region \times group interaction was found. In all subjects, if the TSPO binding status was entered as covariate, a statistically significant difference between groups was found for the medial temporal cortex (Table 2). If only the HABs were included, statistically significant differences between groups were found for the lateral and medial temporal cortex, posterior cingulate, caudate, putamen, thalamus and cerebellum (Table 2). In

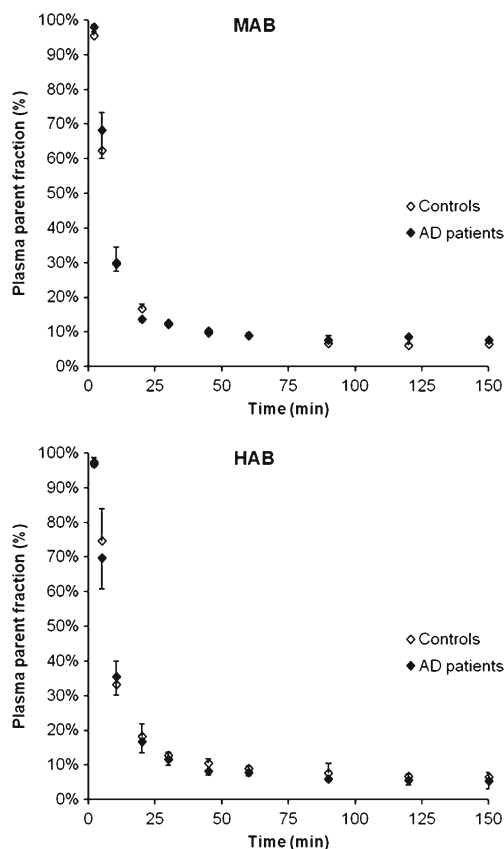
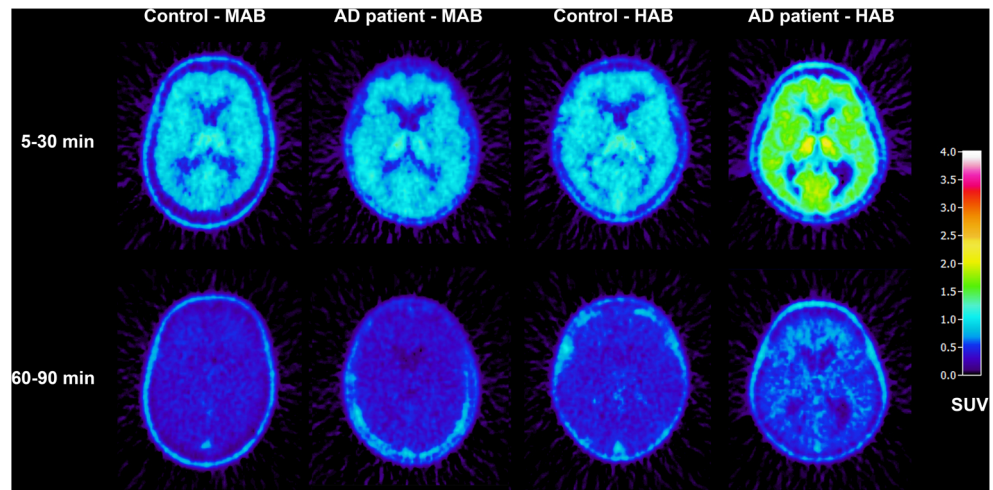


Fig. 1 Mean plasma parent fractions in mixed-affinity binder (MAB) and high-affinity binder (HAB) in controls and AD patients. The error bars represent 1 SD

Fig. 2 Representative SUV images of mixed-affinity binders (MAB) and high-affinity binders (HAB). Transaxial slices at the level of the basal ganglia from two control subjects and two AD patients are shown. Frames between 5 and 30 min (*top row*) and between 60 and 90 min (*bottom row*) were averaged



HABs, the V_T values (mean \pm SD) in these regions were on average 19.5 ± 3.0 % higher in AD patients than in controls, ranging from 15 % higher in the lateral temporal cortex to 24 % in the thalamus (Table 2, Fig. 5 and Supplementary Fig. 5).

Discussion

This study was designed to quantify the binding to TSPO of the novel radioligand [^{18}F]FEMPA in controls and AD patients and to evaluate whether increased TSPO binding in AD could be demonstrated in vivo. The primary outcome measure in this study was V_T estimated using kinetic and Logan GA and the metabolite-corrected arterial input function, since no reference region for TSPO is present in the brain. Since a major source of variability in V_T for all second-generation TSPO radioligands is known to come from the *rs6971*

polymorphism of the TSPO [18], the binding status of the subjects was evaluated using a competition assay with [^3H]PK11195 and PBR28. In a separate work, the binding properties of FEMPA have been tested in human brain tissue samples known to belong to different binder subtypes, and it was found that the ratio in affinity between LABs and HABs was approximately 12 (unpublished data), that is about 4.6 times lower than that of PBR28.

The main finding of this study was that increased in vivo binding of [^{18}F]FEMPA to TSPO in AD patients could be demonstrated if the binding status of the subjects was taken into account and more specifically if only HABs were included. [^{18}F]FEMPA appeared to be a suitable radioligand for in vivo TSPO quantification, displaying good brain uptake, fast wash-out from the brain and relatively fast metabolism. V_T estimated using Logan GA was in very good agreement with V_T estimated using the 2TCM and also showed lower variability in both controls and AD patients.

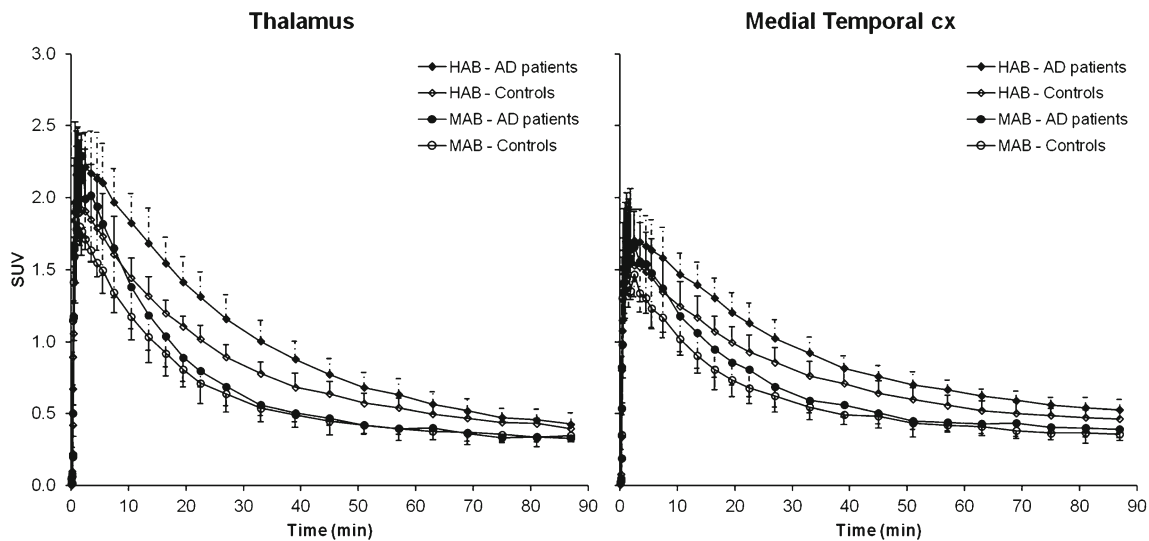


Fig. 3 Mean time-activity curves from mixed-affinity binders (MAB) and high-affinity binders (HAB) (controls and AD patients) for the thalamus and medial temporal cortex. Error bars represent 1 SD

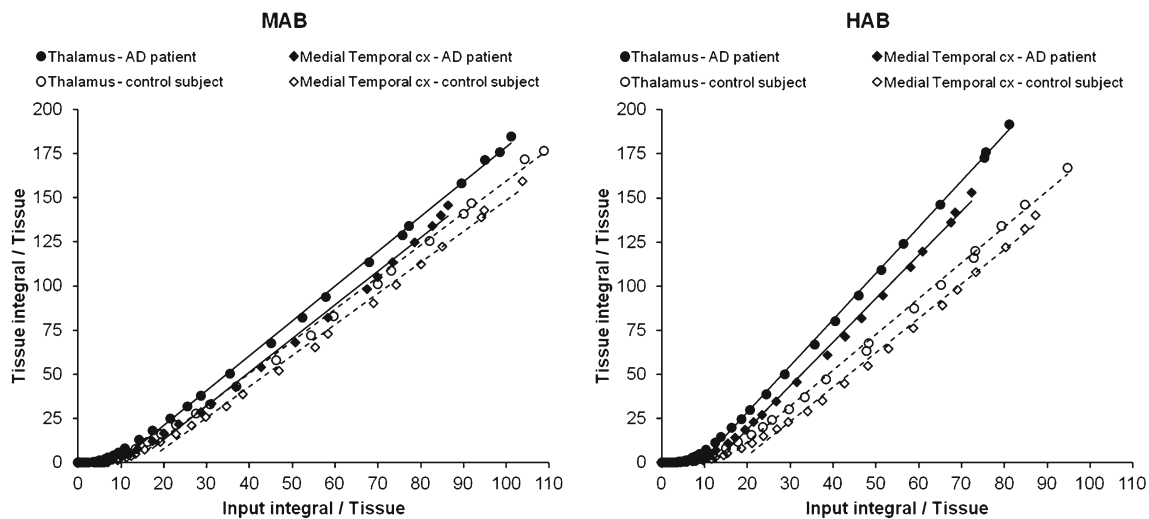


Fig. 4 Representative Logan plots for the thalamus and medial temporal cortex from mixed-affinity binders (MAB) and high-affinity binders (HAB). Data are from the same control subjects and AD patients displayed in Fig. 2

TSPO binding status

In this study the TSPO binding status was examined in a competition assay with [^3H]PK11195 and PBR28. It is known that this assay provides results in agreement with the analysis of the polymorphism of the TSPO gene [22]. The K_i high for the HABs was in good agreement with the K_i value (3.10 ± 5 nM) previously reported by Owen et al. [16]. The K_i high and low values for the MABs were also in agreement with the K_i high and low values (4.0 ± 2.4 and 313 ± 76.8 nM) previously reported [16], although the K_i low value for MABs was more in agreement with the K_i low value previously reported for LABs (188 ± 15.6 nM) [16]. Although in four subjects the protein concentration in the assay was low, leading to a

reduced signal-to-noise ratio, the V_T for HABs was approximately 2.2 times higher than the V_T for MABs, in agreement with the V_T ratio between HABs and MABs found across all subjects, which was approximately 1.5. This ratio is also in agreement with the ratio between HABs and MABs reported for [^{11}C]PBR28 [18].

Quantification of [^{18}F]FEMPA binding to TSPO

The fast kinetic properties of [^{18}F]FEMPA compared with its analogue [^{18}F]FEDAA1106 represent a potential advantage for its clinical use. The kinetic analysis showed that the 2TCM was a suitable model for the quantification of [^{18}F]FEMPA and that V_T estimates obtained with Logan GA were in close

Table 2 V_T values of Logan GA in controls and AD patients (mean \pm SD) with the results of ANOVA

Region	V_T , all subjects			V_T , only HABs		
	Controls	AD patients	F (p value)	Controls	AD patients	F (p value)
Frontal cortex	1.59 \pm 0.40	1.68 \pm 0.63	1.8 (0.202)	1.85 \pm 0.12	2.12 \pm 0.23	4.4 (0.075)
Parietal cortex	1.40 \pm 0.32	1.61 \pm 0.52	4.6 (0.052)	1.61 \pm 0.17	1.86 \pm 0.16	5.2 (0.056)
Lateral temporal cortex	1.50 \pm 0.35	1.61 \pm 0.55	2.8 (0.122)	1.72 \pm 0.10	1.98 \pm 0.17	7.0 (0.033)
Medial temporal cortex	1.64 \pm 0.48	1.88 \pm 0.69	5.1 (0.044)	1.95 \pm 0.12	2.36 \pm 0.18	15.2 (0.006)
Occipital cortex	1.46 \pm 0.35	1.60 \pm 0.52	2.3 (0.154)	1.65 \pm 0.28	1.82 \pm 0.23	1.0 (0.353)
Posterior cingulate	1.62 \pm 0.44	1.86 \pm 0.67	4.1 (0.066)	1.91 \pm 0.10	2.30 \pm 0.24	9.1 (0.020)
Caudate	1.25 \pm 0.33	1.35 \pm 0.49	1.9 (0.193)	1.45 \pm 0.05	1.68 \pm 0.19	6.0 (0.045)
Putamen	1.46 \pm 0.44	1.67 \pm 0.64	3.6 (0.080)	1.73 \pm 0.10	2.10 \pm 0.23	8.9 (0.020)
Thalamus	1.64 \pm 0.48	1.89 \pm 0.75	4.1 (0.064)	1.94 \pm 0.09	2.40 \pm 0.29	9.1 (0.019)
Pons	1.70 \pm 0.50	1.92 \pm 0.80	2.8 (0.121)	2.00 \pm 0.15	2.42 \pm 0.35	5.0 (0.060)
Cerebellum	1.43 \pm 0.35	1.61 \pm 0.60	4.2 (0.064)	1.67 \pm 0.06	2.00 \pm 0.24	6.9 (0.034)
White matter	1.44 \pm 0.44	1.61 \pm 0.66	2.4 (0.146)	1.70 \pm 0.14	2.03 \pm 0.33	3.3 (0.111)

The analysis was conducted in all subjects (HABs and MABs) and in the HAB subjects only (four controls, five AD patients). In the ANOVA conducted in all subjects, the TSPO binding status was included as covariate

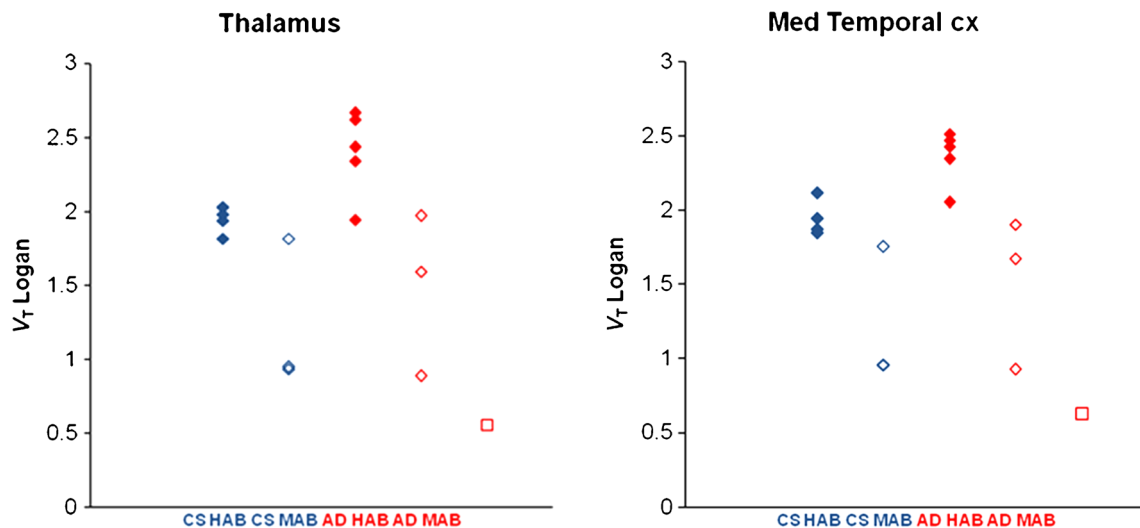


Fig. 5 Scatter plots of V_T values in controls and AD patients (HABs and MABs) for the thalamus and medial temporal cortex. TSPO binding was not analysed in the AD patient represented by the open squares

agreement with the 2TCM. In this study, the study groups comprised only HABs and MABs according to the in vitro binding affinity data. We attempted to estimate the V_T for LABs based on the results for the MABs and HABs (Supplementary Appendix 3). The estimated $V_{T\text{ LAB}}$ was 0.57 ± 0.08 in controls and 0.74 ± 0.28 in AD patients. Interestingly, this value is similar to the lowest V_T value found in the AD patient whose binding status was not analysed and who most likely was a LAB. Assuming that nonspecific binding is similar in HABs, MABs and LABs, and that $V_{\text{ND}} < V_T^{\text{LAB}}$, the binding potential (BP_{ND}) calculated from the distribution volumes [$BP_{\text{ND}} = V_T / (V_{\text{ND}} - 1)$] can be estimated to be at least about 2 in HABs and about 1 in MABs. Interestingly, the estimated BP_{ND} of [^{18}F]FEMPA obtained for HABs and MABs was in agreement with the calculated BP_{ND} for [^{11}C]PBR28 recently found by Owen et al. in a blocking study using the TSPO agonist XBD173 [23].

Increased TSPO binding in AD

We observed that in HABs the increase in [^{18}F]FEMPA binding to the TSPO was between 15 % and 24 %. This finding is in agreement with previous reports using either [^{11}C](R)-PK11195 in AD patients (approximately 20–35 % increased in cortical binding as compared with controls) [9], [^{11}C]DAA1106 in MCI (26 % increase) and AD patients (18 % increase) [13, 14], or [^{11}C]PBR28 in AD patients (38 % increase) [19]. Considering the relatively small sample size of this study, a statistically significant increase in TSPO signal in patients with early AD was detected only after controlling for TSPO binding status, suggesting the potential of [^{18}F]FEMPA for detecting microglial activation in AD.

Additional considerations

The binding of [^{11}C]PBR28 to TSPO has been shown to correlate negatively with MMSE score [19]. We examined the correlation between mean V_T for [^{18}F]FEMPA in the cortical (frontal, temporal, parietal and occipital), limbic (medial temporal cortex and posterior cingulate) and subcortical regions (caudate, putamen and thalamus) and MMSE score, and found a weak nonsignificant negative correlation ($r = -0.37 - -0.41$, $p = 0.12 - 0.17$) when combining data from controls and AD patients (data not shown). The lack of statistically significant correlation might be related to the limited sample size, and further studies are needed to specifically examine the relationship between TSPO binding of [^{18}F]FEMPA and cognitive function in AD.

The PET data were analysed using only a conventional region of interest-based approach. Voxel-based analysis could be useful to identify differences in small areas that can be underestimated by the use of large regions of interest. In this study we did not apply voxel-based analysis because of the limited sample size of both groups and to avoid possible false-positive and false-negative results that can be associated with small samples.

The potential of an ^{18}F -labelled tracer for use in the clinical setting could be improved by the use of a simplified acquisition protocol. However, in the case of [^{18}F]FEMPA, because of the lack of a reference region in the brain arterial input function data are needed to estimate V_T . We did not observe differences in the parent fraction between AD patients and controls, suggesting that the observed differences in V_T do indeed reflect differences in the brain distribution of the tracer. Such differences could be detected only by measuring the brain uptake as SUV. We did observe differences in SUV between the two groups, similar to differences in V_T (data

not shown), which might suggest that SUV could be used as a surrogate outcome measure. However, to validate the potential of SUV as an outcome measure in the clinical setting, additional studies with [¹⁸F]FEMPA in a larger group of AD patients and controls are needed.

Conclusion

[¹⁸F]FEMPA seems to be a suitable radioligand for in vivo imaging and quantification of TSPO in early AD, provided that the TSPO binding status is determined or by including only HABs. Future studies are needed to confirm these findings in a larger cohort of AD patients.

Acknowledgments This study was sponsored by Bayer Healthcare, Berlin, Germany. The work at Turku PET Centre and Karolinska Institutet was supported by the European Union's Seventh Framework Programme (FP7/2007-2013) under grant agreement HEALTH-F2-2011-278850 (INMIND). The compound [¹⁸F]FEMPA is now part of the portfolio of the Piramal Imaging GmbH, Berlin, Germany. The authors thank the staff of the Turku PET Centre, the Karolinska Institutet PET Centre and the Karolinska University Hospital for technical support.

Conflicts of interest Ray Valencia, Marcus Schultze-Mosgau, Andrea Thiele, Sonja Vollmer, Thomas Dyrks, Lutz Lehmann, Tobias Heinrich, Anja Hoffmann were employed by Bayer Healthcare, Berlin, Germany at the time of the study.

Financial support Bayer Healthcare, Berlin, Germany; FP7/2007-2013 HEALTH-F2-2011-278850 (INMIND).

References

1. Wyss-Coray T, Rogers J. Inflammation in Alzheimer disease – a brief review of the basic science and clinical literature. *Cold Spring Harb Perspect Med*. 2012;2:a006346.
2. Rupprecht R, Papadopoulos V, Rammes G, Baghai TC, Fan J, Akula N, et al. Translocator protein (18 kDa) (TSPO) as a therapeutic target for neurological and psychiatric disorders. *Nat Rev Drug Discov*. 2010;9:971–88.
3. Scarf AM, Kassiou M. The translocator protein. *J Nucl Med*. 2011;52:677–80.
4. Bird JL, Izquierdo-Garcia D, Davies JR, Rudd JH, Probst KC, Figg N, et al. Evaluation of translocator protein quantification as a tool for characterising macrophage burden in human carotid atherosclerosis. *Atherosclerosis*. 2010;210:388–91.
5. Cosenza-Nashat M, Zhao ML, Suh HS, Morgan J, Natividad R, Morgello S, et al. Expression of the translocator protein of 18 kDa by microglia, macrophages and astrocytes based on immunohistochemical localization in abnormal human brain. *Neuropathol Appl Neurobiol*. 2009;35:306–28.
6. Kuhlmann AC, Guilarte TR. Cellular and subcellular localization of peripheral benzodiazepine receptors after trimethyltin neurotoxicity. *J Neurochem*. 2000;74:1694–704.
7. Venneti S, Lopresti BJ, Wiley CA. Molecular imaging of microglia/macrophages in the brain. *Glia*. 2013;61:10–23.
8. Cagnin A, Brooks DJ, Kennedy AM, Gunn RN, Myers R, Turkheimer FE, et al. In-vivo measurement of activated microglia in dementia. *Lancet*. 2001;358:461–7.
9. Edison P, Archer HA, Gerhard A, Hinz R, Pavese N, Turkheimer FE, et al. Microglia, amyloid, and cognition in Alzheimer's disease: an [¹¹C](R)PK11195-PET and [¹¹C]PIB-PET study. *Neurobiol Dis*. 2008;32:412–9.
10. Wiley CA, Lopresti BJ, Venneti S, Price J, Klunk WE, DeKosky ST, et al. Carbon 11-labeled Pittsburgh compound B and carbon 11-labeled (R)-PK11195 positron emission tomographic imaging in Alzheimer disease. *Arch Neurol*. 2009;66:60–7.
11. Schuitemaker A, Kropholler MA, Boellaard R, van der Flier WM, Kloet RW, van der Doef TF, et al. Microglial activation in Alzheimer's disease: an (R)-[¹¹C]PK11195 positron emission tomography study. *Neurobiol Aging*. 2013;34:128–36.
12. Dolle F, Luus C, Reynolds A, Kassiou M. Radiolabelled molecules for imaging the translocator protein (18 kDa) using positron emission tomography. *Curr Med Chem*. 2009;16:2899–923.
13. Yasuno F, Ota M, Kosaka J, Ito H, Higuchi M, Doronbekov TK, et al. Increased binding of peripheral benzodiazepine receptor in Alzheimer's disease measured by positron emission tomography with [¹¹C]DAA1106. *Biol Psychiatry*. 2008;64:835–41.
14. Yasuno F, Kosaka J, Ota M, Higuchi M, Ito H, Fujimura Y, et al. Increased binding of peripheral benzodiazepine receptor in mild cognitive impairment-dementia converters measured by positron emission tomography with [¹¹C]DAA1106. *Psychiatry Res*. 2012;203:67–74.
15. Varrone A, Mattsson P, Forsberg A, Takano A, Nag S, Gulyas B, et al. In vivo imaging of the 18-kDa translocator protein (TSPO) with [¹⁸F]FEDAA1106 and PET does not show increased binding in Alzheimer's disease patients. *Eur J Nucl Med Mol Imaging*. 2013;40:921–31.
16. Owen DR, Howell OW, Tang SP, Wells LA, Bennacef I, Bergstrom M, et al. Two binding sites for [³H]PBR28 in human brain: implications for TSPO PET imaging of neuroinflammation. *J Cereb Blood Flow Metab*. 2010;30:1608–18.
17. Owen DR, Gunn RN, Rabiner EA, Bennacef I, Fujita M, Kreisl WC, et al. Mixed-affinity binding in humans with 18-kDa translocator protein ligands. *J Nucl Med*. 2011;52:24–32.
18. Owen DR, Yeo AJ, Gunn RN, Song K, Wadsworth G, Lewis A, et al. An 18-kDa translocator protein (TSPO) polymorphism explains differences in binding affinity of the PET radioligand PBR28. *J Cereb Blood Flow Metab*. 2012;32:1–5.
19. Kreisl WC, Lyoo CH, McGwiler M, Snow J, Jenko KJ, Kimura N, et al. In vivo radioligand binding to translocator protein correlates with severity of Alzheimer's disease. *Brain*. 2013;136:2228–38.
20. McKhann GM, Knopman DS, Chertkow H, Hyman BT, Jack CR Jr, Kawas CH, et al. The diagnosis of dementia due to Alzheimer's disease: recommendations from the National Institute on Aging-Alzheimer's Association workgroups on diagnostic guidelines for Alzheimer's disease. *Alzheimers Dement*. 2011;7:263–9.
21. Wahlund LO, Barkhof F, Fazekas F, Bronge L, Augustin M, Sjogren M, et al. A new rating scale for age-related white matter changes applicable to MRI and CT. *Stroke*. 2001;32:1318–22.
22. Kreisl WC, Jenko KJ, Hines CS, Lyoo CH, Corona W, Morse CL, et al. A genetic polymorphism for translocator protein 18 kDa affects both in vitro and in vivo radioligand binding in human brain to this putative biomarker of neuroinflammation. *J Cereb Blood Flow Metab*. 2013;33:53–8.
23. Owen DR, Guo Q, Kalk NJ, Colasanti A, Kalogiannopoulou D, Dimber R, et al. Determination of [¹¹C]PBR28 binding potential in vivo: a first human TSPO blocking study. *J Cereb Blood Flow Metab*. 2014;34:989–94.